Journal of Magnetic Resonance 195 (2008) 60–66

Contents lists available at ScienceDirect

Journal of Magnetic Resonance

journal homepage: www.elsevier.com/locate/jmr

# Quasioptical study of antiferromagnetic resonance in $YFeO_3$ at submillimeter wavelength under high pulsed magnetic fields

A.A. Mukhin [a,*], A.N. Lobanov [b], M. Goiran [c], J. Leotin [c], A.A. Volkov [a]

[a] A.M. Prokhorov General Physics Institute RAS, Submillimeter Spectroscopy, 38, Vavilov Street, Moscow 119991, Russian Federation
[b] P.N. Lebedev Physical Institute RAS, 53, Leninsky Prosp., Moscow 119991, Russian Federation
[c] Laboratoire National des Champs Magnétiques Pulsés, 143, ave. De Rangueill, Toulouse 31400, France

ARTICLE INFO

*Article history:*
Received 6 July 2007
Revised 20 May 2008
Available online 3 September 2008

*Keywords:*
Antiferromagnetic resonance
High magnetic field
Submillimeter spectroscopy
Polarization
Impurity mode
Orthoferrite

ABSTRACT

Transmission spectra, $T(H)$, of linearly polarized electromagnetic waves through $YFeO_3$, weak ferromagnet, measured at frequencies $\nu$ = 96–1000 GHz in long-pulsed magnetic fields ($H||k||c$-axis, Faraday geometry) exhibit strong rotation of the polarization plane near the quasiferromagnetic AFMR as well as low frequency impurity modes. New ascending impurity branch including five lines was observed at high magnetic field (10–30 T) at 96 GHz and 140 GHz in addition to the known low-field descending impurity branch. Behavior of all the impurity modes assigned to transitions in $^6S_{5/2}$ multiplet of $Fe^{3+}$ "impurity" ions in $c$-sites was described self-consistently by one spin-Hamiltonian. A theoretical calculation of dynamical magnetic susceptibility at AFMR and impurity modes and further simulation of transmission spectra made it possible to describe the main features of the observed spectra $T(H)$. It was found that the $T(H)$ behavior is determined at resonances not only by non-diagonal components of the magnetic susceptibility but also by the anisotropy of the dielectric permittivity ($\varepsilon'_{xx} \neq \varepsilon'_{yy}$), i.e. birefringence.


## 1. Introduction

Rare-earth (R) orthoferrites $RFeO_3$ belong to a wide class of weak ferromagnets exhibiting very interesting magnetic properties related to an existence of different magnetic interactions, spin-reorientation phase transitions, magnetic excitations and many other phenomena (see, for example, [1,2]). Various magnetic resonance modes, both in iron and rare-earth subsystems of $RFeO_3$, were studied by diverse spectroscopic techniques, such as far-infrared spectroscopy [3], neutron scattering [4], Raman scattering [5], microwave magnetic resonance technique [6,7] and quasioptical backward-wave oscillator spectroscopy [8,9].

New possibilities in such investigations could be provided by the quasioptical far-infrared technique combined with high pulsed magnetic fields [10,11]. As a rule, such measurements are performed in Faraday geometry, i.e. for a propagation of the electromagnetic radiation with a wave vector **k** along external magnetic field (**H**), and are accompanied by a rotation of polarization plane and interference effects, especially near magnetic resonance modes (see, for example, [12]). It requires the control of the polarization radiation to account for and interpret these phenomena.

In this work we have used far-infrared lasers and microwave techniques with a quasioptical control of the polarization to study antiferromagnetic resonance (AFMR) and impurity modes in yttrium orthoferrite $YFeO_3$ in high pulsed magnetic fields (up to 40 T) for the Faraday geometry. Besides two AFMR modes (quasiferromagnetic and quasiantiferromagnetic modes, respectively, at $\nu_1 \sim 300$ GHz and $\nu_2 \sim 590$ GHz for 4.2 K [5,8,9]), $YFeO_3$ exhibits at low temperatures ($T < 50$ K) also few impurities modes $\nu_{imp}$ at 255-300 GHz at zero magnetic field [13,9]. Magnetic field applied along the $c$-axis results in softening of the impurity modes, which were assigned to magneto-dipolar transitions in $^6S_{5/2}$ multiplet of $Fe^{3+}$ "impurity" ions in $c$-sites [14]. Such behavior of the impurity modes, representing actually electron paramagnetic resonance in internal exchange and external magnetic fields, could be explained by an opposite direction of the internal effective field and the external one which determines a descending impurity branch for fields below the threshold field $H_0 \sim 15$ T [14] and suggests the existence of an ascending impurity branch for $H > H_0$. The search for such high-field impurity brunch was one of the aims of this work.

## 2. Experimental results

Single crystals of $YFeO_3$ were grown by a floating zone method with radiation heating [15]. The plane-parallel plate of $c$-cut of the orthorhombic crystal (space group $D_{2h}^{16}$—Pbnm) with a transverse size ~7–8 mm and thickness $d$ = 0.993 mm was prepared for the FIR study.

Measurements in a "transmission" scheme were performed by means of far-infrared laser and microwave techniques in pulsed

* Corresponding author. Fax: +7 499 135 2368.
*E-mail address:* mukhin@ran.gpi.ru (A.A. Mukhin).

1090-7807/$ - see front matter © 2008 Elsevier Inc. All rights reserved.
doi:10.1016/j.jmr.2008.08.014

magnetic fields up to 40 T oriented along the weak ferromagnetic moment of the crystal **F**||*c*-axis (Faraday geometry). A control of the polarization was carried out by a wire grid polarizer and an analyzer in a quasioptical cell installed inside the pulsed coil (Fig. 1). To bring the radiation into the channel of the pulsed magnet we used the oversized cylindrical waveguide ($D$ = 6 mm), made of a thin-walled stainless steel. It is well known that the cylindrical waveguide changes the linear polarization of the far infrared and sub-millimeter radiation into the elliptical one. To obtain the linear polarization of the incident and transmitted radiation we used tungsten wire grid polarizers (wire diameter, grid period and aperture of 20 μm, 60 μm and 7 mm, respectively) located close to the sample. These polarizers are effective within the entire range of frequencies (96–1000 GHz) taking into account transmission characteristics of such polarizers reported in Ref. [16]. The cylindrical waveguide was coupled to the open space by means of two fused quartz lenses (focal length ~10 mm). A loss of radiation intensity due to conversion of propagating modes was less than 50% for each side.

Bulk metallic pieces should not be used during measurements in strong pulsed magnetic fields because of heating and vibrations induced by eddy-currents. The sample holder, including the diaphragm, some lenses and polarizer mountings, collets for cylindrical wave-guides—were fabricated of polyetheretherketone polymer **PEEK**™. Internal and external surfaces of the sample holder were covered by 10 μm thin gold film to prevent the radiation propagation around the sample. We used two diaphragms with aperture 4 and 6 mm. No noticeable difference was observed in the measurements performed with the two diaphragms, thus we may conclude, that the focal spot was not exceeding 4 mm in diameter.

To check the applicability of the quasi-optical scheme for polarization measurements we tested the propagation of the radiation without the sample. The radiation passed to the detector through the crossed polarizer and analyzer did not exceed 2–3%, thus indicating the polarization degree better than 97%.

The sample was placed at the center of the coil where the homogeneity of the magnetic field is $10^{-3}$ over 10 mm the coil axis.

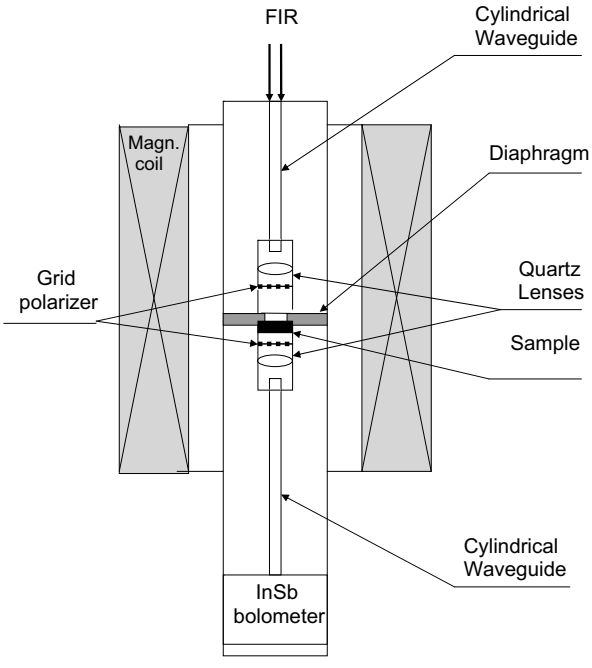


**Fig. 1.** Scheme of the quasioptical cell installed in a 40 T pulsed coil.

Pulsed magnetic field duration was about 0.2 s, the maximum of the field was reached in 80 ms.

The high frequency measurements (above 250 GHz) were carried out using a gas filled Fabry–Perot cavity optically pumped by a $CO_2$ laser, while the low frequency studies were performed by means of semiconductor generators (Gunn diode and avalanche diode). A fast InSb bolometer, set out of the coil was used as a detector.

The peculiarity of the quasi-optical configuration is the appearance of interference of the radiation for plane parallel samples, which results in some complexity of transmission spectra. To avoid this interference the wedge-shaped specimens are usually used. In our coil with a small bore diameter it is difficult to use wedge-shaped samples because of parasitic asymmetrical reflections coming from different elements of the quasioptical cell and sample surface, which give rise to multiple standing waves, obstructing the treatment of the transmitted signal. On the other hand plane parallel samples were used in the frequency domain quasi-optical studies [8,9] for quantitative description of spectra and extracting information on a complex permittivity taking into account multiple interferences. In this work we have also used the plane-parallel samples to provide better theoretical treatment of measured spectra.

The main part of the measurements was carried out for crossed analyzer and polarizer geometry in order to study the effects of the polarization plane rotation. The usual approach to measure the polarization characteristics in magnetic fields includes observation of the transmission in crossed polarizer and analyzer, while the polarizer is aligned along a crystallographic axe of the sample. The polarization plane rotation under magnetic field gives rise to a signal at the detector, thus opening a possibility to adjust the system. In our pulsed field experiment, where the adjustment of the measuring system including the radiation source, wave guide and the quasioptical channel, was possible only without the magnetic field, the orientation of the analyzer and polarizer was chosen close to ±45° with respect to the crystallographic *a*- and *b*-axes in the sample plane. In this case a sufficient signal was detected due to the transformation of the linear polarization to the elliptical one owing to a natural birefringence (i.e., anisotropy of permittivity $\varepsilon'_{xx} \neq \varepsilon'_{yy}$). When the orientation of the crossed polarizer and analyzer was along crystallographic *a*- and *b*-*axes* there were no change of polarization, thus we were not able to adjust the system due to a very weak signal at the detector.

Examples of transmission spectra $T(H)$ near the resonance bands are shown in Figs. 2 and 3 and the dependencies of the observed resonance frequencies as a function of the magnetic field along *c*-axis are displayed in Fig. 4. The increasing high-frequency branch $\nu_1(H)$ represents a known quasiferromagnetic AFMR mode which is excited by the ac magnetic field $h||a$- and *b*-axes in the full range of the applied external magnetic fields $H||c$ [7–9]. The observation of the mode in a crossed analyzer and polarizer configuration suggests a rotation of the polarization plane. The complicated shape of the resonance bands, including multiple picks, indicates significant interference effects inside the line in the plane parallel sample (Fig. 2a–c). We note also a qualitative change of the shape of the resonance bands for different frequencies.

The low frequency branches in Fig. 4 can be identified as impurity modes. The descending branch $\nu_i^-(\mathrm{H})(\mathrm{i} = 1,2,3,4,5)$ including a group of five lines represents the known impurity modes observed in work [14], while the ascending frequencies $\nu_i^+(\mathrm{H})$ is a new impurity branch consisting of also five lines. In the transmission spectra measured without analyzer, the impurity modes look like usual absorption lines while for the crossed analyzer and polarizer geometry the lineshape of the modes changes qualitatively and reveals marked "positive" and "negative" peaks (Fig. 3) resem-

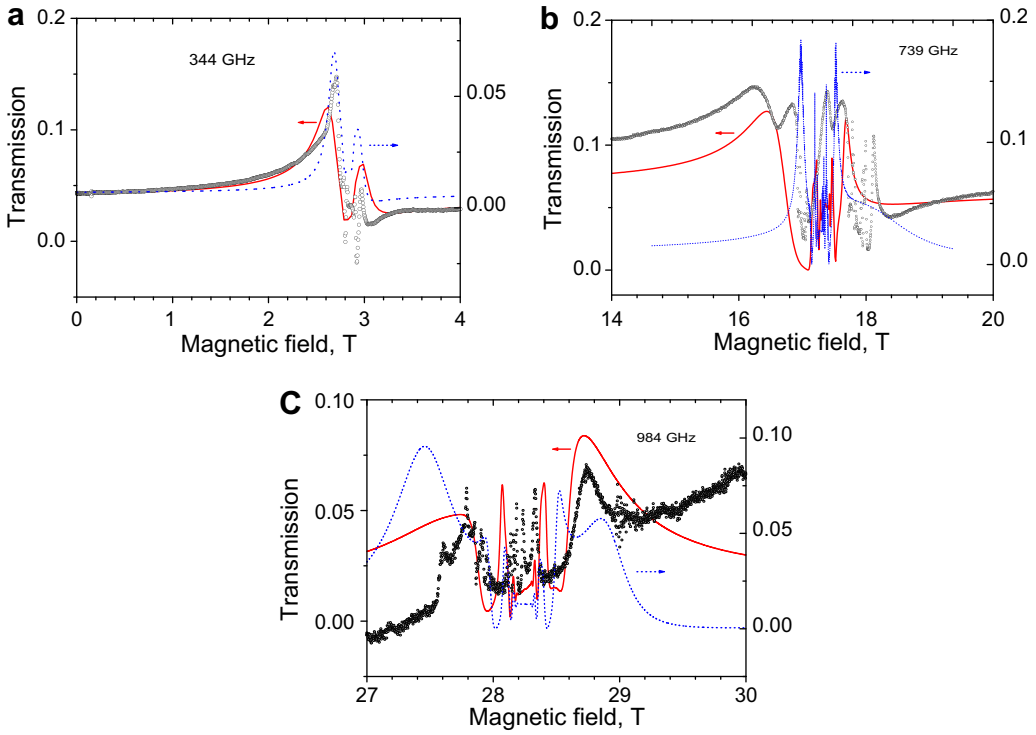


**Fig. 2.** Transmission spectra $T(B)$ of $c$-cut $YFeO_3$ plan-parallel plate of the thickness $d = 0.993$ mm near resonance fields of quasiferromagnetic AFMR mode measured at frequencies 344 GHz (a), 739 GHz (b) and 984 GHz (c) for the temperature $T = 4.2$ K. The measurements were performed for crossed polarizer and analyzer oriented at ~±45° relatively to $a$- and $b$-axes, respectively. Open circles—experiment, dotted and solid lines—theory, respectively, for dielectrically isotropic and anisotropic cases (see text); the experimental spectra initially measured in arbitrary units were scaled then to the theoretical ones. The complicated shape of the resonance bands including a lot of closed picks occurs due to interference of two proper elliptically polarized modes characterized by the refraction indexes $n_{1,2}$ from Eq. (6).

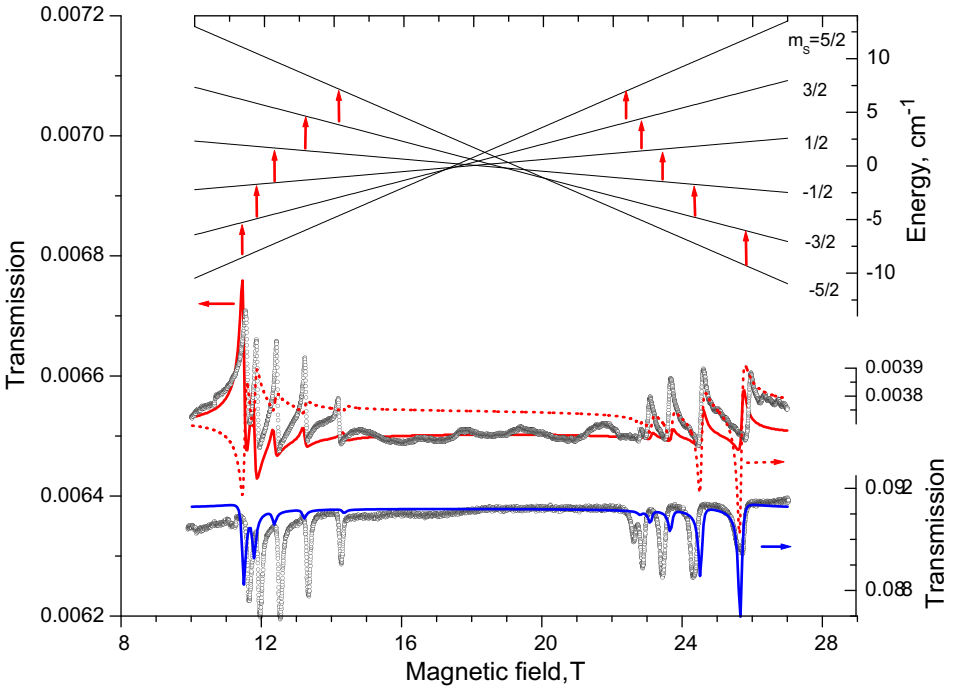


**Fig. 3.** Transmission spectra $T(B)$ of $c$-cut $YFeO_3$ plan-parallel plate of the thickness $d = 0.993$ mm near impurity spin resonances at frequency 96 GHz for the temperature $T = 4.2$ K. The low panel corresponds to the measurements without analyzer and polarizer $e||b$-axis while the middle one—for crossed polarizer and analyzer oriented at ~±45° relatively to $a$- and $b$-axes. Points—experiment, solid and dotted lines—theory, respectively, for dielectrically isotropic and anisotropic cases (see text). Upper panel shows the calculated spectrum of $^6S_{5/2}$ multiplet of $Fe^{3+}$ "impurity" ions in $c$-sites determined by spin-Hamiltonian (9). The arrows indicate the observed transitions.

bling the derivative of the absorption lines. The features observed for the crossed analyzer and polarizer could be considered as indication of a resonance rotation of the polarization plane, which has different signs above and below the corresponding resonance fields resulting in increasing or decreasing transmission. Such behavior of the polarization plane rotation near 300 GHz was observed

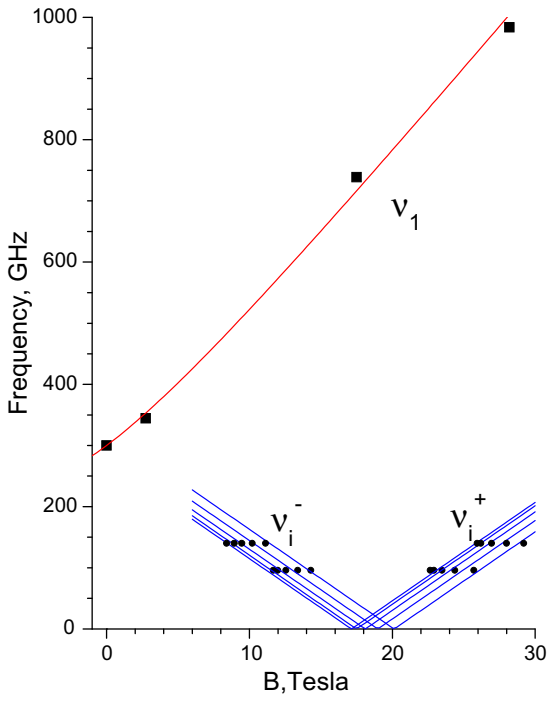


**Fig. 4.** AFMR and impurity resonance frequencies in $YFeO_3$ as a function of magnetic field $B||c$ for $T = 4.2$ K. Points—experiment, lines—theory.

recently in single molecule magnet Mn12ac by means of quasioptical backward oscillator spectroscopy [17]. We note the marked resonance signal despite the low impurity concentration ($c_{imp} \sim 3.5 \times 10^{-4}$ according to Ref. [14]). At temperatures above 40 K the intensity of the impurity resonance modes is significantly reduced due to a change of energy level population of the $Fe^{3+}$ ions in $c$-positions.

## 3. Theory and discussion

In order to describe the observed resonance features near the quasiferromagnetic and impurities modes as well as to estimate the reliability of the used quasioptical scheme for the Faraday geometry we have simulated the transmission spectra taking into account a polarization plane rotation and interference of the radiation inside a plane parallel sample. Tensors of absolute gyrotropic permeability $\hat{\mu}_a(\nu)$ and permittivity $\hat{\varepsilon}_a(\nu)$ in the stable magnetic configuration $F_zG_x$ (in Berto notations) of orthorhombic $YFeO_3$ with a weak ferromagnetic moment **F** aligned along $c$-axis and an antiferromagnetic moment **G**$||a$-axis have the form:

$$\hat{\mu}_a \equiv \mu_0\hat{\mu} = \mu_0\begin{pmatrix} \mu_{xx} & i\mu_{xy} & 0 \\ -i\mu_{xy} & \mu_{yy} & 0 \\ 0 & 0 & \mu_{zz} \end{pmatrix}, \quad \hat{\varepsilon}_a \equiv \varepsilon_0\hat{\varepsilon} = \varepsilon_0\begin{pmatrix} \varepsilon_{xx} & i\varepsilon_{xy} & 0 \\ -i\varepsilon_{xy} & \varepsilon_{yy} & 0 \\ 0 & 0 & \varepsilon_{zz} \end{pmatrix}. \tag{1}$$

where $\hat{\mu}$ and $\hat{\varepsilon}$ are the relative permeability and permittivity, respectively, and $\mu_0$ and $\varepsilon_0$ are the magnetic and electric constants. Frequency and magnetic field dependence of the permeability at the AFMR modes can be found from equations of motion (Landau–Lifshits equations) for the dynamic variables **F** and **G** using the non-equilibrium thermodynamic potential (see, for example, [9])

$$\Phi(\mathbf{F},\mathbf{G},\mathbf{H}) = 1/2A\mathbf{F}^2 - d_1F_xG_z - d_3F_zG_x - \mu_0M_0\mathbf{FH} + 1/2K_{ac}G_z^2 + 1/2K_{ab}G_y^2, \tag{2}$$

where $A$ and $d_1 \approx -d_3 = d$ are isotropic and antisymmetric Dzyaloshinskii–Morija exchange constants, respectively. $K_{ac}$ and $K_{ab}$ are the anisotropy constants in $ac$- and $ab$-planes, respectively, $M_0$ is the sublattice magnetization. The resonance frequencies of the quasiferromagnetic mode $\omega_1$, of the quasiantiferromagnetic mode $\omega_2$ and the dynamic magnetic susceptibility $\chi_{\alpha\beta}$ (permittivity $\mu_{\alpha\beta} = \delta_{\alpha\beta} + \chi_{\alpha\beta}$) are [9]

$$\begin{aligned} &\omega_1 \equiv 2\pi\nu_1 = [\omega_{01}^2 + \gamma H_z(H_D + H_z)]^{1/2}, \\ &\omega_2 \equiv 2\pi\nu_2 = [\omega_{02}^2 + \gamma H_D H_z]^{1/2}, \quad \chi_{xx} = \chi_{rot}L_1(\omega), \\ &\chi_{yy} = \chi_\perp L_1(\omega), \quad \chi_{xy} = (\omega/\omega_1)G_x^0(\chi_{xx}\,\chi_{yy})^{1/2}, \\ &\chi_{zz} = \chi_\perp L_2(\omega), \end{aligned} \tag{3}$$

where $\omega_{01} = \gamma(2H_EK_{ac}/M_0)^{1/2}$, $\omega_{02} = \gamma(2H_EK_{ab}/M_0 + H_D^2)^{1/2}$ are the AFMR frequencies at zero field, $\chi_\perp = M_0/2H_E$ and $\chi_{rot} = \chi_\perp[\gamma(H_D + H_z)/\omega_1]^2$ are the perpendicular and rotational susceptibilities, respectively, $\mu_0H_E = A/2M_0$ and $\mu_0H_D = d/M_0$ are the isotropic and antisymmetric Dzyaloshinskii–Morija exchange fields, respectively, $\gamma \approx 2\mu_B/\hbar$ is the gyromagnetic ratio for $Fe^{3+}$ spins, $G_x^0 = \pm 1$ is an equilibrium antiferromagnetic moment, whose sign is determined by the sign of the weak ferromagnetic moment (and external magnetic field) along $c$-axis. The functions $L_{1,2}(\omega) = \omega_{1,2}^2/(\omega_{1,2}^2 - \omega^2 + i\omega\Delta\omega_{1,2})$ determine the Lorentzian AFMR lineshape, where $\Delta\omega_{1,2}$ is the corresponding linewidth.

Electromagnetic wave $\mathbf{E}_{tr}$ transmitted through a plane-parallel layer (plate) can be determined by a two dimensional transmission matrix $\hat{T}$ (Jones matrix), $\mathbf{E}_{tr} = \hat{T}\mathbf{E}_{inc}$, where $\mathbf{E}_{inc}$ is a normally incident radiation [18]. The Jones matrix of the $YFeO_3$ $c$-cut plane-parallel plate was calculated using Maxwell equations taking into account the corresponding gyrotropic permeability $\hat{\mu}(\nu)$ and permittivity $\hat{\varepsilon}(\nu)$ as well as boundary conditions, reflection and interference (see also [12]):

$$\hat{T} = (\hat{1} + \hat{R})[\hat{1} - (\hat{S}\hat{R})^2]^{-1}\hat{S}(\hat{1} - \hat{R}), \tag{4}$$

where $\hat{S}$ is a matrix characterizing a propagation of waves in an infinite media for a distance $d$ and $\hat{R}$ is a reflectivity matrix for a vacuum-media boundary. The propagation matrix:

$$\hat{S} = \hat{P}^{-1}\begin{pmatrix} \exp(-ik_1d) & 0 \\ 0 & \exp(-ik_2d) \end{pmatrix}\hat{P} \tag{5}$$

is found by solving the wave equation for an electric field **E** in a media with the given $\hat{\mu}(\nu)$ and $\hat{\varepsilon}(\nu)$ tensors and involves contributions of two normal elliptically polarized (in a common case) modes characterized by the eigenwave vectors $k_{1,2} = (2\pi\nu/c)n_{1,2}$ and refractive indexes:

$$n_{1,2} = [\Delta_{\varepsilon\mu} \pm (\Delta_{\varepsilon\mu}^2 - \Delta_\varepsilon\Delta_\mu)^{1/2}]^{1/2}, \tag{6}$$

and eigenvectors $\mathbf{e}_1 = (e_{1x}, e_{1y})$ and $\mathbf{e}_2 = (e_{2x}, e_{2y})$ defining the projection matrix $\hat{P}(P_{xx} = e_{2y}/\Delta_e, P_{xy} = -e_{2x}/\Delta_e, P_{yx} = -e_{1y}/\Delta_e, P_{yy} = e_{1x}/\Delta_e)$ and the inverse matrix $\hat{P}^{-1}(P_{xx}^{-1} = e_{1x}, P_{xy}^{-1} = e_{2x}, P_{yx}^{-1} = e_{1y}, P_{yy}^{-1} = e_{2y})$, where $\Delta_{\varepsilon\mu} = (\varepsilon_{xx}\mu_{yy} + \varepsilon_{yy}\ \mu_{xx} + 2\varepsilon_{xy}\mu_{xy})/2$, $\Delta_\varepsilon = \varepsilon_{xx}\varepsilon_{yy} - \varepsilon_{xy}^2$, $\Delta_\mu = \mu_{xx}\mu_{yy} - \mu_{xy}^2$, $\Delta_e = e_{1x}\,e_{2y} - e_{1y}\,e_{2x}$ and $c = 1/\sqrt{\varepsilon_0\mu_0}$ is the electrodynamic constants coinciding with the light velocity in a vacuum. The reflection matrix is:

$$\hat{R} = (\hat{n} + \hat{\tilde{\mu}})^{-1}(\hat{n} - \hat{\tilde{\mu}}) \tag{7}$$

where:

$$\hat{n} = \hat{P}^{-1}\begin{pmatrix} n_1 & 0 \\ 0 & n_2 \end{pmatrix}\hat{P}, \quad \hat{\tilde{\mu}} = \begin{pmatrix} \mu_{yy} & i\mu_{xy} \\ -i\mu_{xy} & \mu_{xx} \end{pmatrix}. \tag{8}$$

For a non-gyrotropic media ($\varepsilon_{xy} = \mu_{xy} = 0$), the above formulae are reduced to the known Fresnel equations [19].

Using Eqs. (1)–(8) we have simulated the observed transmission spectra near the quasiferromagnetic mode which are shown in

Fig. 2 by solid lines. The theory reflects the qualitative features inside the lines related to the interference of two proper propagating modes having different field-dependent refractive indexes $n_{1,2}(H_z)$. However, we were not able to describe all the details of the spectra in the frame of the used model of infinite layer and plane wave approximation. It indicates that this approach is not completely suitable for our experiment, where the transversal dimensions of the diaphragm aperture are not much greater than the wavelength and the beam shape is far from pure plane wave. However, taking into account of these effects would be too complicated, so we have used the above-mentioned approximation. The calculations were performed for the magnetic parameters $\nu_{10} \equiv \omega_{10}/2\pi \approx 300$ GHz, $\Delta\nu_1 \equiv \Delta\omega_1/2\pi \approx 0.6$ GHz, $\mu_0 H_E \approx 640$ T, $\mu_0 H_D \approx 13$ T and permittivity $\varepsilon_{xy} = 0, \varepsilon''_{xx,yy} = 0.04, \varepsilon'_{xx} = 21{-}23, \varepsilon'_{yy} = 19{-}21$, where the low and high values of the $\varepsilon'_{xx,yy}$ correspond to the frequencies from ~100 GHz up to ~1000 GHz, respectively. It was found that the simulated resonance rotation of the polarization plane amounts to several tens of degrees near $\nu_1$ and that the $T(H)$ behavior is determined not only by a sample thickness and the magnetic susceptibility but also by permittivity including its anisotropy ($\varepsilon'_{xx} \neq \varepsilon'_{yy}$), i.e. birefringence. In order to clarify the role of various parameters of $YFeO_3$ in the appearance of the complex AFMR lineshape we have simulated the transmission spectra as a function of the sample (optical) thickness in the cases of isotropic ($\varepsilon'_{xx} = \varepsilon_{y'y} = 21.8$) and anisotropic ($\varepsilon'_{xx} = 22.8, \varepsilon'_{yy} = 20.8$) dielectric constant. The results are shown in Fig. 5 at the left and right panels, respectively (the polarization is similar to Fig. 2).

It is obvious that a resonance line having a single pick at small thickness becomes more complicated and exhibits additional interference picks which number is increased for the larger thickness. For the small thickness (0.05 mm) the lineshape is very similar both in isotropic and anisotropic cases, however, with the increasing of the thickness one can see qualitatively difference between the lineshape in the isotropic and anisotropic cases. To show more clearly the role of the dielectric anisotropy in the observed AFMR resonance spectra we have also added in the Fig. 2 the spectra calculated for dielectrically isotropic case with $\varepsilon' = (\varepsilon'_{xx} + \varepsilon'_{yy})/2$ (dotted lines) which demonstrates a qualitative difference from the corresponding anisotropic case and disagreement with the experiment that indicates the effect of the natural birefringence in the

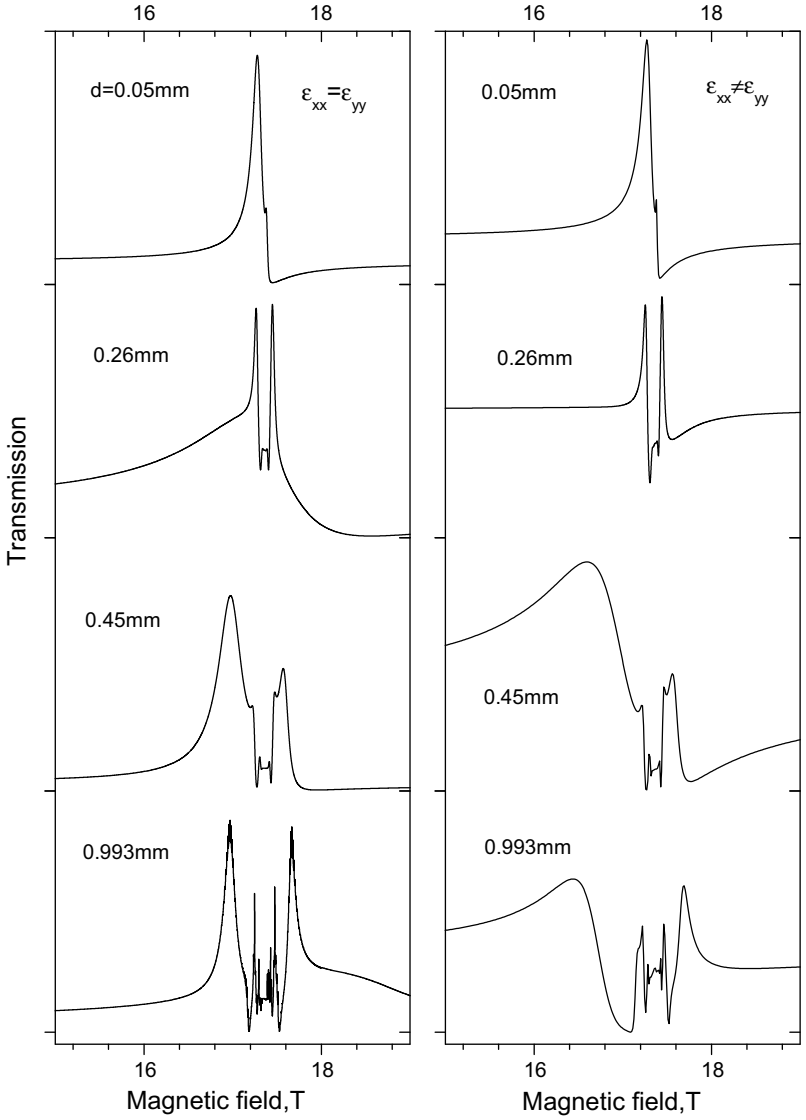


**Fig. 5.** Evolution of the AFMR lineshape as a function of the sample thickness simulated for the dielectrically isotropic, $\varepsilon_{xx'} = \varepsilon_{y'y}$ (left panel) and anisotropic, $\varepsilon'_{xx} \neq \varepsilon'_{yy}$ (right panel) cases. The calculations of the transmission were performed for the frequency 739 GHz and Faraday geometry with the crossed polarizer and analyzer used in the experiments. The data show qualitative change of the AFMR lineshape not only with increasing of the sample thickness but also its sensitivity to the anisotropy of permittivity (i.e. natural birefringence) for sufficiently thick sample.

observed phenomena. The high sensitivity of the spectra near the antiferromagnetic resonance to the permittivity allows, in principle, to determine not only parameters of the AFMR modes but also to get some information on dielectric constants, their anisotropy and frequency dependence. In particular, the found birefringence $\varepsilon'_{xx} - \varepsilon'_{yy} \approx 2{-}2.3$ corresponds to the $YFeO_3$ data obtained by studies in the quasioptical frequency domain [12].

The dependence of the AFMR frequency $\nu_1(H_z)$ calculated for above parameters (see Eq. (3)) describes the corresponding experiment data in the full range of the fields (Fig. 4).

To analyze the experimental data for the impurity modes of the $Fe^{3+}$ "impurity" with spins $S = 5/2$ in $c$-sites of the host crystals we used the spin-Hamiltonian:

$$\mathrm{H}_{\mathrm{eff}} = \mathrm{g}\mu_{\mathrm{B}}\mathbf{B}_{\mathrm{eff}}\mathbf{S} + \mathrm{DS}_z^2 + \mathrm{aS}_z^3, \tag{9}$$

where $\mathbf{B}_{\mathrm{eff}} \approx \mu_0(\mathbf{H} + \lambda_{\mathrm{F}}\mathbf{F} + \hat{\lambda}_{\mathrm{G}}\mathbf{G})$ is the effective field determined by the external magnetic field $\mathbf{H}$ and the exchange field from the $Fe^{3+}$ spins of the host matrix, which includes the isotropic ($\lambda_{\mathrm{F}}\mathbf{F}$) and anisotropic ($\hat{\lambda}_{\mathrm{G}}\mathbf{G}$) contributions. The $\mathrm{DS}_z^2$ term represents a crystal field and $\mathrm{a}\cdot\mathrm{S}_z^3$ is a contribution from a non-Heisenberg part of impurity-host exchange appearing in a high order perturbation theory and being an odd function of the host spins (see [20]). Similar spin-Hamiltonian (in a simpler form) was used in Ref. [14] to describe the descending branch of the impurity modes.

In the equilibrium state for the host $Fe^{3+}$ spins with $F_z^0 \approx (H_z + H_D G_x^0)/2H_E$, $G_x^0 = \pm 1$ the energy levels $E_n$ of the spin-Hamiltonian $H_{\mathrm{eff}}^0$ (9) are $E_m = g\mu_B m\mu_0[H_{\mathrm{eff}0}^z + (1+k)H_z] + Dm^2 + am^3$, where $m = -5/2,\ -3/2, \ldots, 5/2$, $\mathrm{k} = \lambda_{\mathrm{F}}/2\mathrm{H}_{\mathrm{E}}$ and $H_{\mathrm{eff}0}^z = (\lambda_F H_D/2H_E + \lambda_G^{zx})G_x^0$ is the effective field at H = 0. The magnetodipolar transitions are allowed between neighboring states $|m\rangle \to |m \pm 1\rangle$, thus determining the five transitions shown in the insert of Fig. 3.

The dynamic susceptibility $\hat{\chi}_{\mathrm{imp}}(\omega)$ of the impurity $Fe^{3+}$ ions with respect to oscillating external magnetic field $\mathbf{h}$ can be expressed as (see, for example, [21]):

$$(\hat{\chi}_{\mathrm{imp}})_{\alpha\beta} = 2N_{\mathrm{imp}} \sum_{\substack{n,m \\ n\neq m}} \rho_m \left[\frac{\mathrm{Re}(\mu_{nm}^{\alpha}\mu_{mn}^{\beta})}{E_n - E_m} + \frac{i\omega}{\omega_{nm}} \frac{\mathrm{Im}(\mu_{nm}^{\alpha}\mu_{mn}^{\beta})}{E_n - E_m}\right] L_{mn}(\omega) \tag{10}$$

where $\omega_{nm} = (E_n - E_m)/\hbar$ and $\mu_{nm}^{\alpha} = g\mu_B < n|S_\alpha|m >$ are the frequencies and the matrix elements of magnetic moment between $|\mathrm{n}\rangle$ and $|m\rangle$ states of the $\mathrm{H}_{\mathrm{eff}}^0$, $\rho_m = \exp(-E_m/k_BT)/\sum_n \exp(-E_n/k_BT)$ are populations of the impurity ion states, $\mathrm{L}_{\mathrm{nm}}(\omega) = \omega_{\mathrm{nm}}^2/(\omega_{\mathrm{nm}}^2 - \omega^2 + \mathrm{i}\omega\Delta\omega_{\mathrm{nm}})$ is the Lorentzian lineshape function with a linewidth $\Delta\omega_{\mathrm{nm}}$, $\mathrm{N}_{\mathrm{imp}}$ is a number of the impurities ions and $\alpha, \beta = x, y, z$.

Taking into account a contribution of the host $Fe^{3+}$ spins to a dynamical response of the impurity subsystem determined by the oscillating parts $\sim\Delta\mathbf{F}$ and $\sim\Delta\mathbf{G}$ in $\mathbf{H}_{\mathrm{eff}}$, i.e. $\mathbf{m}_{\mathrm{imp}} = \hat{\chi}_{\mathrm{imp}}(\mathbf{h} + \lambda_F\Delta\mathbf{F} + \hat{\lambda}_{\mathrm{G}}\Delta\mathbf{G})$ as well as similar contribution of the impurity ions to the response of the host $Fe^{3+}$ subsystem, i.e. $\mathbf{m}_{\mathrm{Fe}} = \hat{\chi}_{\mathrm{Fe}}(\mathbf{h} + \lambda_{\mathrm{F}}\mathbf{m}_{\mathrm{imp}})$ it is possible to find the total magnetization $\mathbf{m} \equiv \mathbf{m}_{\mathrm{Fe}} + \mathbf{m}_{\mathrm{imp}} = \hat{\chi}\mathbf{h}$ and express the total susceptibility $\hat{\chi}$ in the form:

$$\hat{\chi} \approx \hat{\chi}_{\mathrm{Fe}} + \hat{\chi}_{\mathrm{imp}} + \tilde{\lambda}_F(\hat{\chi}_{\mathrm{imp}}\hat{\chi}_{\mathrm{Fe}} + \hat{\chi}_{\mathrm{Fe}}\hat{\chi}_{\mathrm{imp}}) + \tilde{\lambda}_{\mathrm{Fe}}^2\hat{\chi}_{\mathrm{Fe}}\hat{\chi}_{\mathrm{imp}}\hat{\chi}_{\mathrm{Fe}}, \tag{11}$$

where $\tilde{\lambda}_{\mathrm{Fe}} = \lambda_{\mathrm{Fe}}/M_0$ and $\hat{\chi}_{\mathrm{Fe}}$ and $\hat{\chi}_{\mathrm{imp}}$ are determined by Eqs. (4) and (10), respectively. The Eq. (11) was derived in a linear approximation on a concentration of the impurity ions $c_{\mathrm{imp}}$ as well as by neglecting the anisotropic exchange field, $\hat{\lambda}_{\mathrm{G}}\Delta\mathbf{G}$, for sake of simplicity. Near the quasiferromagnetic mode the response (11) gives practically the same result as the pure $\hat{\chi}_{\mathrm{Fe}}$ susceptibility due to a small $c_{\mathrm{imp}}$, while at the impurity mode frequencies the contribution of the dynamical exchange fields of the host matrix is not negligible. Results of the simulation of the transmission spectra near the impurity modes and their resonance frequencies field dependencies are shown by solid lines in Figs. 3 and 4, respectively. The parameters of the spin-Hamiltonian (9) $\mu_0 H_{\mathrm{eff}0}^z = -10.9$ T, $\mathrm{k} = -0.396$ ($\mu_0\lambda_{\mathrm{F}} = -506$ T), $D = 0.19$ cm$^{-1}$, $a = 0.026$ cm$^{-1}$ were found by fitting few resonance fields for 96 GHz; the linewidths $\Delta\nu_{\mathrm{nm}}$ were equaled 0.7 GHz for all transitions and the impurity concentration was chosen $3.5 \times 10^{-4}$ according to Ref. [14]. In a whole we note a reasonable agreement between the theory and experiment for both descending and ascending impurity modes as well as for the resonances lineshape. The calculated spectra demonstrate the excellent reproduction of the mode's lineshape for both spectra: without analyzer and with crossed analyzer and polarizer (Fig. 3). The spectrum corresponding to the dielectrically isotropic case with $\varepsilon'_{xx} = \varepsilon'_{yy}$ (dotted line in the middle panel of Fig. 3) exhibits noticeable difference as compared with the anisotropic case thus indicating the role of the natural birefringence similar to the AFMR spectra at Fig. 2. The resonance change of polarization plane orientation near the impurity modes is about or less than 0.5 degrees.

The theoretical dependencies of the resonance frequencies (Fig. 4) also correspond to the experimental data; they were calculated for $\mu_0 H_{\mathrm{eff}0}^z = -10.4$ T, $\mathrm{k} = -0.425$ ($\mu_0\lambda_{\mathrm{F}} = -544$ T), $D = 0.2$ cm$^{-1}$, $a = 0.024$ cm$^{-1}$ determined by fitting resonance fields both for 96 GHz and 140 GHz which are closed to the cited above values. Some deviation of the experiment points from the theory could arise due to some additional (non-diagonal) terms in the impurity spin-Hamiltonian (9) which mix the pure $|m\rangle$ states and avoid the energy level crossing near 17–20 T where the external field compensates the internal exchange one. Besides, the observed relations between intensities of the impurity modes inside the both branches $\nu_{\mathrm{i}}^{\pm}(\mathrm{H})$ (Fig. 3) indicate higher populations of the excited impurity states compared to the Boltzmann equilibrium populations $\rho_{\mathrm{m}}$, suggesting thus an appearance of non-equilibrium populations of the impurity states in a pulsed field due to a longitudinal relaxation.

## 4. Conclusion

The performed high magnetic field FIR studies of the $YFeO_3$ transmission spectra $T(H)$ in the Faraday geometry with a quasioptical control of the polarization revealed a noticeable polarization plane rotation at quasiferromagnetic AFMR and low frequency impurity modes. New ascending impurity branch including five lines was observed under high magnetic fields (10–30 T) at 96–140 GHz in addition to the known low-field descending impurity branch. Behavior of the all "impurity" modes assigned to the transitions inside $^6S_{5/2}$ multiplet of $Fe^{3+}$ ions in $c$-sites was described self-consistently by one spin-Hamiltonian. A theoretical calculation of dynamical magnetic susceptibility at AFMR and impurity modes and further simulation of transmission spectra made it possible to describe the main features of the observed spectra $T(H)$ related to the polarization plane rotation and interference. It was found a noticeable role of the dielectric anisotropy ($\varepsilon'_{xx} \neq \varepsilon'_{yy}$), i.e. birefringence in the studied phenomena in addition to the gyrotropic (non-diagonal) contribution to the permeability.

## Acknowledgments

This work was supported in part by the ECONET Program (France), International Science and Technology Center and Russian Foundation for Basic Researches (No. 06-02-17514).

## Appendix A. Supplementary data

Supplementary data associated with this article can be found, in the online version, at doi:10.1016/j.jmr.2008.08.014.

## References


[1] R.L. White, Review of recent work on the magnetic and spectroscopic properties of the rare-earth orthoferrites, J. Appl. Phys. 40 (1969) 1061–1069.
[2] K.P. Belov, A.K. Zvezdin, A.M. Kadomtseva, R.Z. Levitin, Orientational Transitions in Rare-Earth Magnetics, Nauka, Moscow, 1979.
[3] K.B. Aring, A.J. Sievers, Role of the ytterbium spins in the spin reorientation in $YbFeO_3$, J. Appl. Phys. 41 (1970) 1197–1198.
[4] S.M. Shapiro, J.D. Axe, J.P. Remeika, Neutron-scattering studies of spin waves in rare-earth orthoferrites, Phys. Rev. B 10 (1974) 2014–2021.
[5] R.M. White, R.J. Nemanich, C. Herring, Light scattering from magnetic excitations in orthoferrites, Phys. Rev. B 25 (1982) 1822–1836.
[6] R.C. LeCraw, R. Wolfe, E.M. Gyorgy, F.B. Hagedorn, T.C. Hensel, J.P. Remeika, Microwave absorption near the reorientation temperature in rare earth orthoferrites, J. Appl. Phys. 39 (1968) 1019–1020.
[7] A.M. Balbashov, A.G. Berezin, Yu.M. Gufan, G.S. Kolyadko, P.Yu. Marchukov, E.G. Rudashevsky, Soft mode and energy gap in the spin wave spectrum at second order reorientation phase transition. AFMR in $YFeO_3$, Sov. Phys. JETP 66 (1987) 174–189.
[8] A.A. Volkov, Yu.G. Goncharov, G.V. Kozlov, K.N. Kocharyan, S.P. Lebedev, A.S. Prokhorov, A.M. Prokhorov, Measurement of magnetic spectrum of $YFeO_3$ by the method of submillimeter dielectric spectroscopy, JETP Lett. 39 (1984) 166–169.
[9] A.M. Balbashov, G.V. Kozlov, A.A. Mukhin, A.S. Prokhorov, Submillimeter spectroscopy of antiferromagnetic dielectrics: rare-earth orthoferrites, in: G. Srinivasan, A. Slavin (Eds.), the book High Frequency Processes in Magnetic Materials, Part I, World Scientific, Singapore, 1995, pp. 56–98 (chapter 2).
[10] J.L. Martin, M. Goiran, Z. Golacki, J. Leotin, S. Askenazy, Far-infrared spin resonance in the II–VI diluted magnetic semiconductors $Zn_{1-x}Mn_xSe$, $Cd_{1-x}Mn_xSe$, and $Zn_{1-x}Co_xS$, Phys. Rev. B 50 (1994) 10680–10693.
[11] A.A. Mukhin, A.E. Egoyan, A. Wittlin, M.E.J. Boonman, A.M. Balbashov, I.Yu. Parsegov, Far-infrared study of field-induced phase transitions in $Y_{0.5}Lu_{0.5}FeO_3$ and $HoFeO_3$ orthoferrites, Phys. B: Condens. Matter 211 (1995) 108–111.
[12] A.A. Mukhin, V.D. Travkin, S.P. Lebedev, A.S. Prokhorov, A.M. Balbashov, I.Yu. Parsegov, Magnetooptical effects at submillimetre wavelengths near afmr in $YFeO_3$, J. Phys. IV (Colloque) 7 (1997) 713–714.
[13] A.M. Balbashov, A.A. Volkov, G.V. Kozlov, S.P. Lebedev, A.S. Prokhorov, Peculiarities of $YFeO_3$ submillimeter spectra at low temperatures, Fiz. Tverd. Tela (Solid States Phys.) 27 (1985) 270–272.
[14] A.M. Balbashov, A.G. Berezin, Ju.V. Bobryshev, P.Yu. Marchukov, I.V. Nikolaev, E.G. Rudashevsky, J. Paches, L. Pust, Orthogonal magnetic impurity in antiferromagnet $YFeO_3$ single crystal: magnetic resonance and magnetization measurements, J. Magn. Magn. Mater. 104–107 (1992) 1037–1038.
[15] A.M. Balbashov, S.K. Egorov, Apparatus for growth of single crystals of oxide compounds by floating zone melting with radiation heating, J. Cryst. Growth 52 (1981) 498–504.
[16] W.G. Chambers, A.E. Costley, T.J. Parker, Characteristic curves for the spectroscopic performance of free-standing wire grids at millimeter and submillimeter wavelengths, Int. J. Infrared Millimeter Waves 9 (2) (1988) 157–172.
[17] J. van Slageren, S. Vongtragool, A. Mukhin, B. Gorshunov, M. Dressel, Terahertz Faraday effect in single molecule magnets, Phys. Rev. B 72 (2005) 020401 (R)–020405 (R).
[18] A.K. Zvezdin, V.A. Kotov, Modern Magnetooptics and Magnetooptical Materials, Institute of Physics, Bristol, 1997.
[19] M. Born, E. Wolf, Principles of Optics, Pergamon, Oxford, 1986.
[20] G. Mischler, P. Carrara, Y. Merle D'Aubigne, Impurity spin resonance of $Mn^{2+}$ in antiferromagnetic $FeBr_2$, Phys. Rev. B 15 (1977) 1568–1577.
[21] P. Fulder, in: K.A. Gsechneidner, Tr. Eyring, L. Eyring (Eds.), Handbook on Physics and Chemistry of Rare-Earths, North-Holland, Amsterdam, 1979.